ISSN 1063-7761, Journal of Experimental and Theoretical Physics, 2017, Vol. 124, No. 2, pp. 304–310. © Pleiades Publishing, Inc., 2017.
Original Russian Text © V.N. Nikiforov, A.N. Ignatenko, V.Yu. Irkhin, 2017, published in Zhurnal Eksperimental'noi i Teoreticheskoi Fiziki, 2017, Vol. 151, No. 2, pp. 356–363.

Size and Surface Effects on the Magnetism of Magnetite and Maghemite Nanoparticles

V. N. Nikiforov[a]*, A. N. Ignatenko[b], and V. Yu. Irkhin[b]
[a] *Moscow State University, Moscow, 119991 Russia*
[b] *Mikheev Institute of Metal Physics, Ural Branch, Russian Academy of Sciences, ul. S. Kovalevskoi 18, Yekaterinburg, 620990 Russia*
**e-mail: pppnvn@yandex.ru*

Received July 20, 2016

Abstract—The size effects of magnetite and maghemite nanoparticles on their magnetic properties (magnetic moment, Curie temperature, blocking temperature, etc.) have been investigated. Magnetic separation and centrifugation of an aqueous solution of nanoparticles were used for their separation into fractions; their sizes were measured by atomic force microscopy, dynamic light scattering, and electron microscopy. A change in the size leads to a change in the Curie temperature and magnetic moment per formula unit. Both native nanoparticles and those covered with a bioresorbable layer have been considered. The magnetic properties have been calculated by the Monte Carlo method for the classical Heisenberg model with various bulk and surface magnetic moments.

DOI: 10.1134/S1063776117010046

1. INTRODUCTION

The first magnetic material known to humanity, magnetite, still remains in many respects mysterious owing to the complex interactions of spin, orbital, and charge degrees of freedom [1].

Apart from magnetite, maghemite (γ-Fe_2O_3), which also has the crystal structure of spinel, belongs to the magnetic iron oxides. The existence of a planar nanophase ε-Fe_2O_3 has also been discussed in recent years [2].

In magnetite one Fe^{3+} ion occupies a tetrahedral site, while each of the two other ions, Fe^{3+} and Fe^{2+}, occupies octahedral sites. Owing to the cation and vacancy ordering, maghemite can have a tetragonal superstructure. The formulas for magnetite and maghemite are $Fe^{3+}[Fe^{3+}Fe^{2+}]O_4$ and $Fe^{3+}[Fe^{3+}_{0.33}]O_4$, respectively. Usually, there is a continuous series between (suboxidized) magnetite and the state completely oxidized to maghemite.

Maghemite is a very common mineral on the Earth's surface. It is also found in corrosion products and proteins, is used in medicine as an agent for drug delivery [3] and in nuclear magnetic resonance tomography [4], and is widely applied as a magnetic recording medium [5].

Maghemite is unstable: it loses its magnetic properties and transforms into hematite (α-Fe_2O_3) as the temperature rises (when heated, they form a continuous metastable magnetic solid solution). The transformation temperature depends on prehistory: in slightly oxidized samples its value is near 300°C, while in more oxidized ones it is above 450°C [6]. Its value is also affected by the particle size, water content, and stoichiometry [7].

Magnetite and maghemite nanoparticles are widely used in information recording and storage systems, biological studies, and medical tests (hyperthermia).

Nanomagnetite is used in magnetic hyperthermia as an efficient material at low frequencies (below 1 MHz [8]), because the Neel easy axis–hard axis flipping mechanism is realized [4]. The production of magnetic nanoparticles with a Curie temperature in the range 45–70°C allows a self-regulating heating of tumor tissues in a variable magnetic field to be achieved [1, 9]. These nanoparticles are very attractive because of their low toxicity and good magnetic properties.

Small nanoparticle sizes strongly affect many characteristics of the materials being discussed: for example, the magnetic anisotropy can be noticeably larger than that for a bulk sample, while the saturation magnetization, on the contrary, is smaller. The Curie temperatures for nanoparticles with sizes of the order of a few nanometers can differ from T_C for bulk samples by hundreds of degrees [10]. We will provide the results of our studies of magnetic properties for iron oxide nanoparticles and will present the corresponding theoretical discussion.

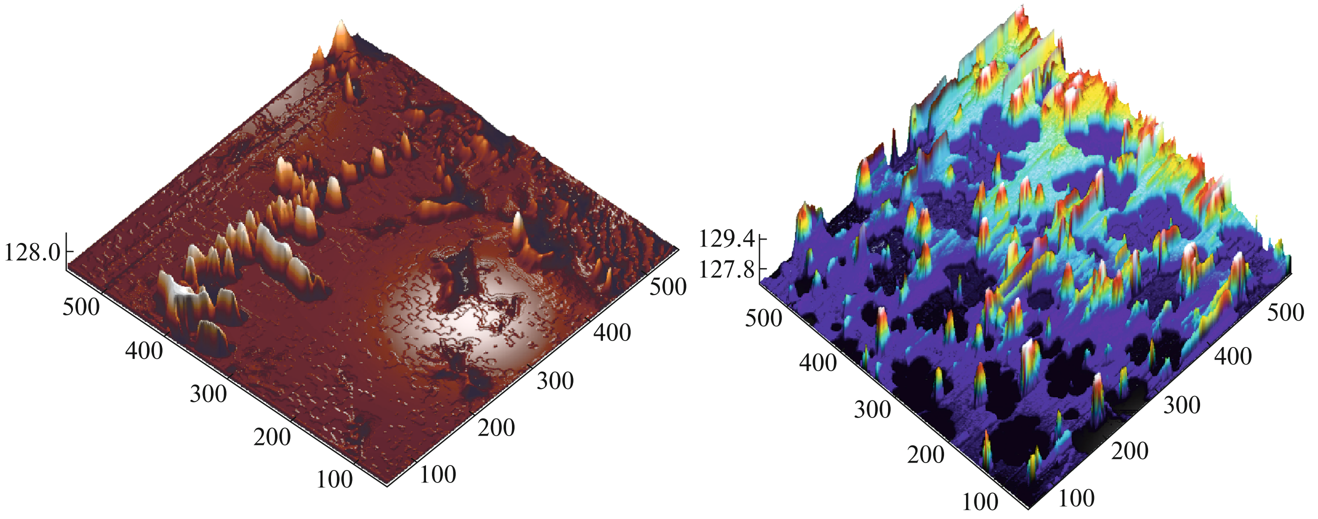

Fig. 1. (Color online) Results of our AFM study (the contact mode, Nano Wizard 3) of magnetite nanoparticles of various fractions with different mean nanoparticle sizes (the mean sizes for the left and right pictures are different). Magnetic separation and centrifugation were used to separate the nanoparticles into fractions with different sizes (in the range from 4 to 22 nm).

2. RESULTS OF OUR MEASUREMENTS

We investigated both native and dextran-passivated magnetite nanoparticles and maghemite nanoparticles synthesized by coprecipitation [11] and aerosol pyrolysis [12]. In aqueous base the magnetite nanoparticles were produced by the sol–gel method.

The nanoparticle size was controlled by dynamic light scattering (DLS), X-ray diffraction (XRD), atomic force microscopy (AFM), and scanning electron microscopy (SEM). Using magnetic separation and centrifugation [13], we managed to separate the nanoparticles into fractions with different sizes in the range from 4 to 22 nm.

Figure 1 shows the results of our AFM study of two fractions of magnetite nanoparticles with different mean sizes.

Since the native magnetic nanoparticles aggregate after their synthesis fairly rapidly (in 20–60 min), they were covered with a passivating coating (dextran, glass, polymers). Their properties can apparently be determined both by the central part, a core, that gives distinct reflexes on electron microscopy and by the shell, a near-surface region of the order of a few nanometers, that gives a “halo” on electron microscopy. This allows the core–shell model to be used. The core and the shell can have different magnetocrystalline anisotropies (K_v and K_s), different magnetic moments per formula unit, and different lattice parameters, which affects significantly the distribution pattern of the magnetic moments.

The core–shell structure is apparently formed in all nanoparticles with sizes of the order of a few nanometers, irrespective of whether they are dressed by a passivating coating or not. The disrupted surface layer of a magnetic nanoparticle can be similar in nature to amorphized magnetite [14]. In addition, the cubic lattice parameter for magnetite nanoparticles with a size of a few nanometers can differ from that for bulk samples, which also has an analogy with amorphous materials [14]. The form and type of coating can affect a number of physical properties of nanoparticles, in particular, their magnetic properties.

The Curie point of the samples was determined from the temperature dependence of the SQUID magnetization in weak magnetic fields (20 mT). We found the second derivatives of the temperature dependences of the saturation magnetization $J_s(T)$. The thermomagnetic curves $J_s(T)$ were measured with a magnetometer by the Curie balance technique in a magnetic field of 7 T in the temperature range 20–500°C. All samples have superparamagnetic dependences of their magnetization on magnetic field without hysteresis.

The magnetic moment per nanoparticle can be calculated by analyzing the magnetization curves $M(H)$ for a solution of superparamagnetic nanoparticles using the Langevin formula. The dependence of the magnetic moment per formula unit for the magnetite nanoparticles in a dextran shell decreases with increasing number of formula units N (Fig. 2).

The linear dependence $\Delta M(N^{-1/3})$ (see the inset in Fig. 2) fits into the phenomenological Weizsäcker formula, which can be used by analogy with nuclear physics [15] (for a discussion of our numerical results see Section 3). The presence of two linear segments may be indicative of a change in the character of the nanoparticle coating (for example, its magnetic prop-

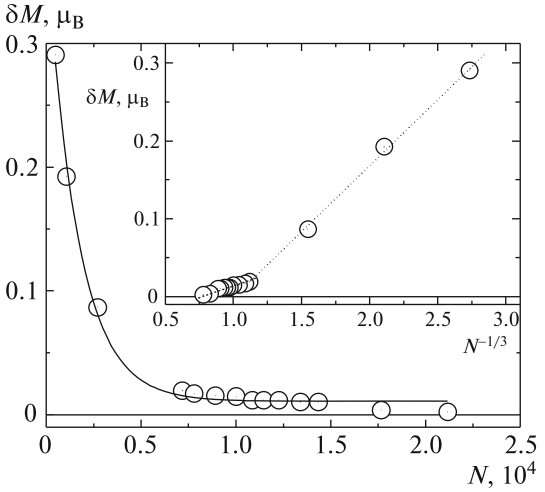

Fig. 2. Deviation of the specific (per formula unit) magnetic moment of magnetite nanoparticles in a dextran shell of diameter 4–22 nm from its value corresponding to a bulk sample determined from the Langevin formula, $T = 300$ K, the measurement was made in fields up to 0.5 T.

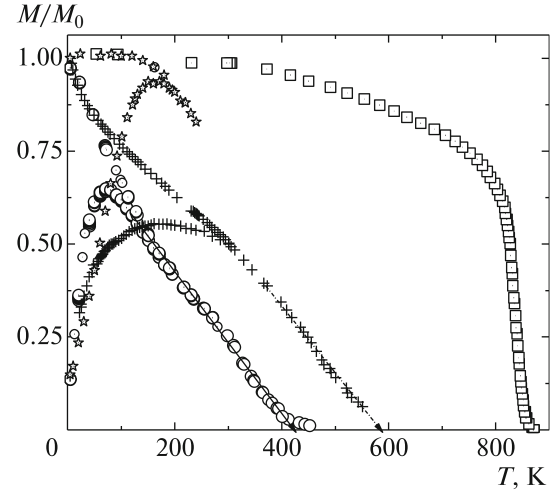

Fig. 3. Temperature dependence of the relative ZFC/FC magnetization for bulk magnetite samples ($M_0 = 2.1$ A m^2 kg^{-1}, squares) and dextran-coated magnetite nanoparticles with sizes of 10 ($M_0 = 0.86$ A m^2 kg^{-1}, stars), 6 ($M_0 = 0.83$ A m^2 kg^{-1}, crosses), and less than 6 ($M_0 = 0.76$ A m^2 kg^{-1}, circles) nm. The experiment was performed with a SQUID magnetometer; $B = 2.27$ mT.

erties, thickness, etc.) when passing to very small sizes of about 4 nm.

The magnetite nanoparticles in a polymer matrix have a more complex dependence of the magnetic moment on the nanoparticle dimeter [15]. Thus, the magnetic moment of the nanoparticle core interacts with the magnetic moment of the shell located under the “coat” of the passivating (biocompatible) nanoparticle coating, which, in turn, depends on the type and form of the coat.

The interaction between the two magnetic systems of the core and the shell, just as two sublattices in a ferromagnet, can lead to experimentally observable effects:

(1) A decreasing, close to $T^{3/2}$, or linear dependence of the magnetization in a wide temperature range, 77–350 K (see Fig. 3), transforming into Smith’s law [16] that differs sharply from the dependence $M(T)$ for bulk magnetite.

(2) A Curie temperature dependent on the nanoparticle size (see Fig. 4). The temperature dependences of the nanoparticle magnetic moment for both magnetite and maghemite (see Figs. 3 and 5) give T_C considerably lower than those for bulk samples (the mass of the single crystals is ~1 g). Note that when the Fe^{3+} ions in magnetite are substituted by gadolinium ions with larger magnetic moments, this dependence of T_C weakens significantly (Fig. 4).

(3) The dependence of the blocking temperature on the type of coating and the nanoparticle preparation process (whether a magnetic field was applied during the passivation and drying of nanoparticles or not; see Fig. 6). The data on the blocking temperature for magnetite nanoparticles 10 nm in size with various coatings obtained with a SQUID magnetometer are collected in [15].

Comparison of the curves describing the Curie temperature drops with decreasing size in weak (H ~ 20 mT) and strong (H ~ 7 T) fields (Fig. 7) shows their qualitative similarity. However, the size effect is more pronounced for the experiments in strong fields, which may be due to the difference between the magnetic field dependences for the core and the shell.

For the investigated maghemite nanoparticles $T_C = 545$ K (with an error of 10 K), which is considerably lower than that for bulk magnetite, $T_C = 918$ K [18]. The dependence $M(T)$ is nearly linear at low temperatures and transforms into a power law at temperatures above 250 K. At the same time, no sharp ferromagnet–paramagnet transition typical of bulk samples is observed at the Curie point. We found a significant difference between the magnetic properties of maghemite in the form of nanoparticles and a bulk material. This effect is apparently attributable to the competition of superexchange interactions between the Fe^{3+} ions at the tetrahedral and octahedral crystallographic sites under conditions of very small sizes, of the order of a few atomic layers, which is confirmed by Monte Carlo simulations [17].

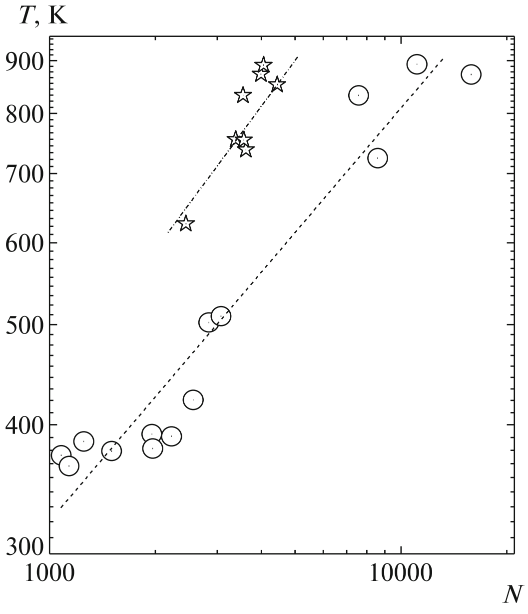

Fig. 4. Size dependence of the Curie temperature in a double logarithmic scale for magnetite nanoparticles (circles) and nanoparticles with 10% of the Fe^{3+} ions substituted by Cd^{3+} ions (stars), N is the number of formula units in a nanoparticle.

3. NUMERICAL SIMULATIONS AND DISCUSSION OF RESULTS

To draw theoretical conclusions and to obtain estimates, we performed Monte Carlo simulations. Models with magnetic moments, exchange integrals, and magnetic anisotropy constants changed on the surface [19] can be used in considering the magnetism of nanoparticles. To study in detail the dependence of magnetic properties on the particle size for magnetite (on which we have more detailed experimental data), we used the simplified model of spherical nanoparticles in which the atoms in the surface layer (coat) and in the bulk were nonequivalent: the ratios of their magnetic moments **s** could be both larger and smaller than unity. We considered the Hamiltonian of the classical isotropic Heisenberg model:

$$H = -\frac{J}{2}\sum_{i,j}\mathbf{S}_i \cdot \mathbf{S}_j,$$

where i and j denote the nearest neighbors of a spherical nanoparticle, $\mathbf{S}_i$ are the magnetic moments of the atoms. Thus, we neglect the details of the magnetic moment formation in a magnetite unit cell. The magnetic moments of the nanoparticle core atoms are normalized to unity, $|\mathbf{S}_i| = 1$, while for the surface atoms $|\mathbf{S}_i| = s$, where s can differ from unity (the possible difference between the exchange parameters in the bulk and on the surface can be taken into account by rescaling s).

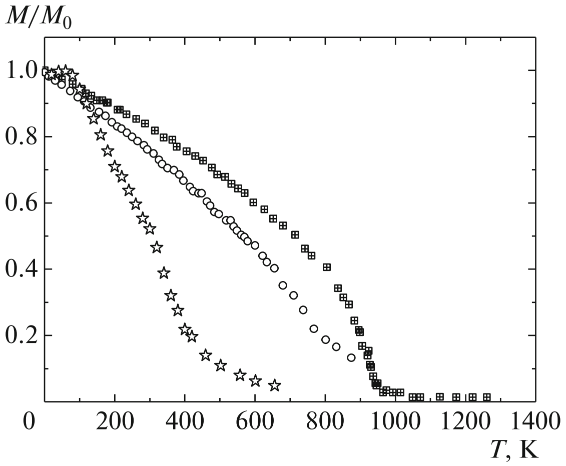

Fig. 5. Temperature dependences of the magnetic moment for the investigated maghemite nanoparticles with a size of 4 nm (stars), M_0 = 2.5 A m^2 kg^{-1}; the data on bulk maghemite (squares) and maghemite nanoparticles (circles) from [17] in relative units are also presented.

A spherical nanoparticle of radius R could be defined by the inequality $|\mathbf{r}_i| < R$, where $\mathbf{r}_i$ are the sites of a simple cubic lattice. Accordingly, a monoatomic surface layer would be defined by the inequality $R - a < |\mathbf{r}_i| < R$, where a is the lattice constant. However, this definition leads to strong "geometrical" oscillations of the number of surface atoms N_s (see Fig. 8), which makes the subsequent interpretation of the Monte Carlo results difficult. To reduce the N_s fluctuations, we modified this definition by substituting $R \rightarrow R + x$

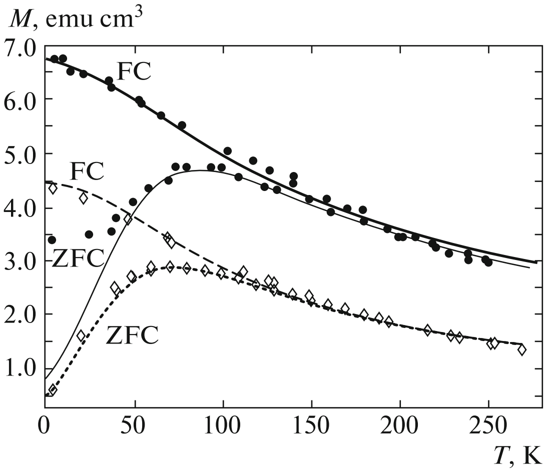

Fig. 6. Curves of the dependence of the magnetic moment on ZFC/FC field for magnetite nanoparticles in polyvinyl films dried in a magnetic field (diamonds) and without any field (circles). The experiment was performed with a SQUID magnetometer; H = 24 Oe, $m_{Fe_3O_4}$ = 45 mg.

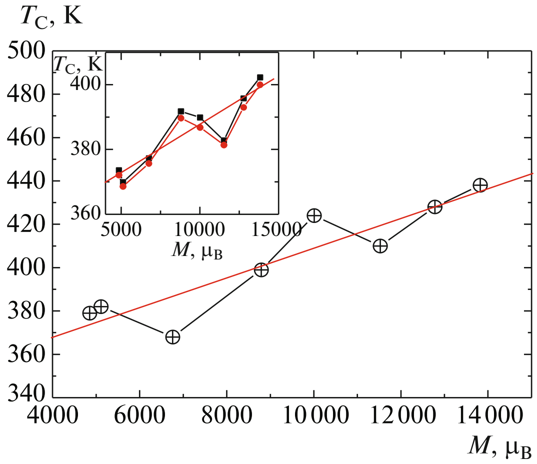

Fig. 7. (Color online) Dependence of the Curie temperature on the magnetic moment of a magnetite nanoparticle determined using the Langevin formula from our magnetization measurements in weak applied fields (20 mT, the inset) and strong fields (7 T). The experiment was performed with a SQUID magnetometer and a balance magnetometer: $T_{\text{balance}}(\text{K}) = 340 + 0.007M(\mu_B)$, T_{SQUID} (K) = $358 + 0.003M(\mu_B)$.

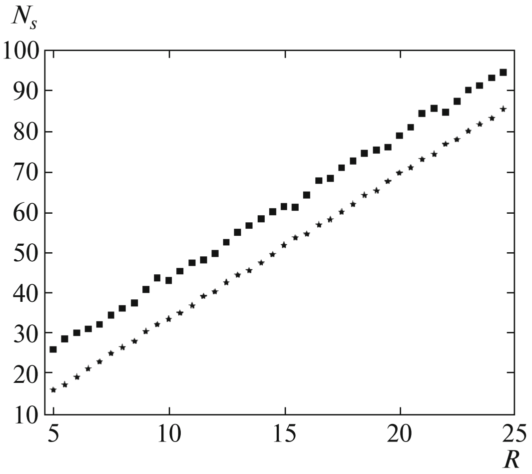

Fig. 8. Dependence of the number of surface atoms N_s on the radius of a spherical nanoparticle defined by the simple inequality $|\mathbf{r}_i| < R$ (squares) and the inequality with a random variable (stars).

in it, where x is a normally distributed random variable with zero mean and standard deviation $\sigma = 0.2$. It can be seen from Fig. 8 that randomness leads to a smoothing of the dependence of N_s on the nanoparticle radius.

To perform our simulations, we implemented the heat bath algorithm [20] based on the ALPS library [21]. The corresponding results on the dependence of the total magnetic moment and Curie temperature of a nanoparticle on the number N of atoms are presented in Figs. 9 and 10 for various values of the parameter s.

It can be seen from Fig. 9 that in the case of identical atoms on the surface and in the bulk ($s = 1$), the finite-size effects per se cannot give a noticeable dependence of the magnetic moment on N for $N > 1000$. At s different from unity the magnetic moment decreases ($s > 1$) or increases ($s < 1$) with growing N. In the latter case, the dependence $\mu(N)$ is consistent with Fig. 2, with the calculated dependences of the magnetic moment being in qualitative agreement with the predictions of the Weizsäcker model ($\mu(N) = a + b/N^{1/3}$) [15].

The Curie temperature of our finite system (see Fig. 10) was determined as the temperature at which the magnetic moment fluctuations were strongest. As a measure of these fluctuations we used the susceptibility $\langle\mu^2\rangle - \langle|\mu|\rangle^2$, where μ is the total magnetic moment. The dependence of the Curie temperature on N can be fairly strong: T_C increases at $s \le 1$ and decreases at $s > 1$ with growing N. The dependence of T_C on N turns out to be stronger than the dependence of the magnetic moment.

It is somewhat unusual that the dependence of the Curie temperature on N is nonmonotonic at $s > 1$. This nonmonotonic dependence may result from the competition of the following two factors: the surface atoms have a smaller number of nearest neighbors, but, at the same time, their magnetic moment is larger, which favors the magnetic order. Despite the fact that the maximal N reached in our calculations is smaller than the number of formula units in real nanoparticles, we

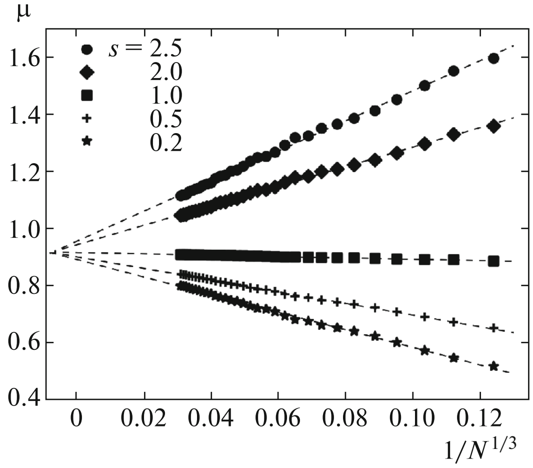

Fig. 9. Total magnetic moment of a nanoparticle normalized to one formula unit versus $1/N^{1/3}$ (N is the number of formula units) for spherical nanoparticles with various surface magnetic moments (s) and temperature $T = 0.3J$. The dashed lines indicate a linear fit; $\mu(N) \approx a + b/N^{1/3}$.

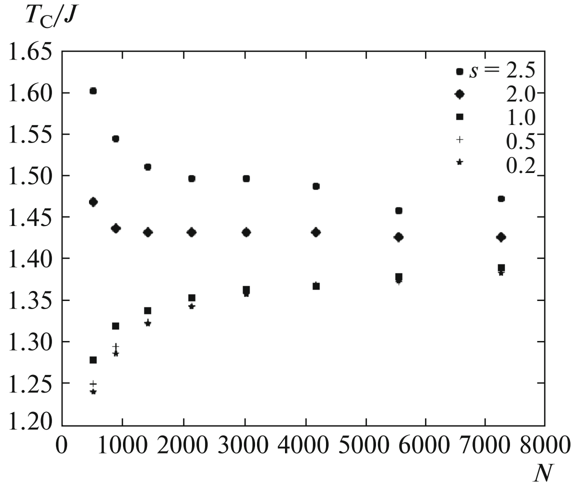

Fig. 10. Curie temperature versus number of atoms in a spherical particle at various s.

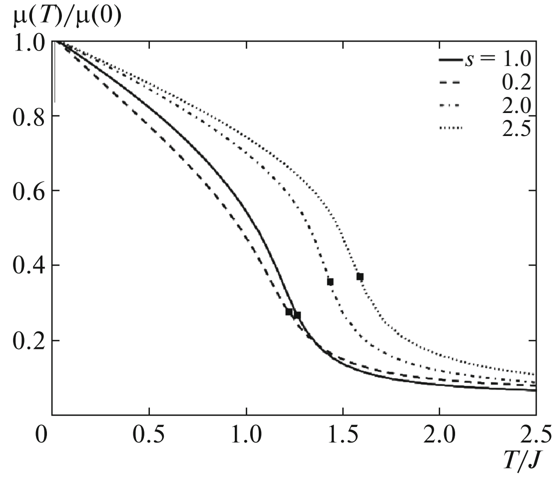

Fig. 11. Typical temperature dependences of the magnetic moment of a nanoparticle containing $N = 515$ formula units with various surface magnetic moments (s).

have qualitative agreement between the simulation and experimental results.

The presence of antiparallel sublattices in the magnetic structure of magnetite makes the temperature behavior of the magnetization more complicated, leading to its nonmonotonicity [1]. This makes a theoretical analysis difficult. However, the Curie temperature can be judged using extrapolation from the spin wave region.

As is shown in Fig. 11, the dependence of the magnetic moment is linear at low temperatures, just as for a classical infinite system (in the quantum case, this behavior changes but is not reduced to the standard Bloch law $T^{3/2}$ [22, 23]); nevertheless, the coefficient characterizing this linear dependence changes significantly with s. For finite systems the temperature dependence of the magnetic moment also changes due to the reduced mean number of nearest neighbors at the boundary [22] and surface anisotropy effects [24, 25].

Note that the temperature behavior of the magnetic moment for nanoparticles will be significantly different than that in the spin wave theory (SWT). For example, the actual Curie temperature can be considerably lower than that in the SWT. This resembles the situation in infinite layered magnets, where the self-consistent spin wave theory (SSWT) predicts a reduction in T_C by 30–50% relative to its value in the SWT [26, 27]. At the same time, the SSWT overestimates T_C compared to the results of Monte Carlo simulations (see, e.g., Fig. 5 in [28]). A further reduction in T_C can be achieved in field-theoretic approaches, which are particularly efficient in the case of low T_C [27].

Thus, our Monte Carlo simulations show that a significant reduction in the Curie temperature of ferromagnetic nanoparticles occurs at a size of ~1000 formula units. In addition, the particle surface coating exerts a significant influence on T_C (Fig. 10).

The magnetic properties of maghemite nanoparticles were numerically studied in [17] by the Monte Carlo method based on a three-dimensional classical Heisenberg model with anisotropy. The structure of spinel with free boundary conditions was simulated more specifically to take into account the surface effect on the characteristics of a nanoparticle with a diameter of ~3 nm. The results show a significant reduction in the Curie temperature of nanoparticles compared to the data obtained for bulk maghemite, from 1000 to ~800 K, in qualitative agreement with our results on the temperature behavior of the magnetization.

4. CONCLUSIONS

Under systematic control of the sizes of nanoparticles we produced the fractions of their aqueous solutions by the separation method. This allowed us to investigate the size effects of magnetite and maghemite nanoparticles on their magnetic properties, because all of the investigated fractions were synthesized by a single method.

We obtained both experimental and theoretical (calculated by the Monte Carlo method) temperature dependences of the magnetic characteristics of magnetite nanoparticles with various sizes and performed a comparison with a bulk Fe_3O_4 sample.

The magnetism of magnetite nanoparticles is determined not only by their sizes but also by their coating-dependent surface spin states, with both increasing and decreasing dependences of the specific (per Fe_3O_4 formula unit) magnetic moment on the number of magnetic atoms being possible.

ACKNOWLEDGMENTS

This work was performed with the State assignment of the Federal Agency for Scientific Organizations (the "Electron" theme; no. 01201463326).

REGERENCES

1. K. P. Belov, Phys. Usp. **36**, 380 (1993).
2. M. Gich, I. Fina, A. Morelli, F. Sanchez, M. Alexe, J. Gazquez, J. Fontcuberta, and A. Roig, Adv. Mater. **26**, 4645 (2014).
3. H. Skaat and S. Margel, Biochem. Biophys. Res. Comm. **386**, 645 (2009).
4. V. N. Nikiforov and E. Yu. Filinova, in *Magnetic Nanoparticles,* Ed. by S. P. Gubin (Wiley-VCH, Weinheim, 2009).
5. F. Jorgensen, *The Complete Handbook of Magnetic Recording* (McGraw–Hill, New York, 1996).
6. C. M. Keefer and P. N. Shive, Earth Planet. Sci. Lett. **51**, 199 (1980).
7. O. Ozdemir, Phys. Earth Planet. Inter. **65**, 125 (1990).
8. V. N. Nikiforov, Russ. Phys. J. **50**, 913 (2007).
9. I. Brezovich, W. J. Atkinson, and D. P. Chakraborty, Med. Phys. **11**, 145 (1984).
10. V. N. Nikiforov, Yu. A. Koksharov, S. N. Polyakov, A. P. Malakho, A. V. Volkov, M. A. Moskvina, G. B. Khomutov, and V. Yu. Irkhin, J. Alloys Compd. **569**, 58 (2013).
11. T. N. Brusentsova, V. D. Kuznetsov, and V. N. Nikiforov, Med. Fiz. **3** (27), 58 (2005).
12. A. E. Chekanova, T. Sorkina, V. N. Nikiforov, A. L. Dubov, G. A. Davydova, I. I. Selezneva, E. A. Goodilin, L. A. Trusov, V. V. Korolev, I. M. Aref'ev, I. V. Perminova, and Y. D. Tretyakov, Mendeleev Comm. **19**, 1 (2009).
13. I. V. Beketov, A. P. Safronov, A. I. Medvedev, J. Alonso, G. V. Kurlyandskaya, and S. M. Bhagat, AIP Adv. **2**, 022154 (2012).
14. H. Pascard and F. Studer, J. Phys. IV **7** [C1], 211 (1997).
15. V. N. Nikiforov et al., arXiv:1206.6985v1.
16. S. V. Vonsovskii, *Magnetism* (Nauka, Moscow, 1971; Wiley, New York, 1971).
17. J. Restrepo, Y. Labaye, and J. M. Greneche, Rev. Soc. Colomb. Fis. **38**, 1559 (2006).
18. X. M. Liu, J. Shaw, J. Z. Jiang, J. Bloemendal, P. Hesse, T. Rolph, and X. G. Mao, China Earth Sci. **53**, 1153 (2010).
19. J. Mazo-Zuluaga, J. Restrepo, and J. Mejia-Lopez, J. Appl. Phys. **103**, 113906 (2008).
20. D. Loison, C. L. Qin, K. D. Schotte, and X. F. Jin, Eur. Phys. J. B **41**, 395 (2004).
21. B. Bauer et al. (ALPS Collab.) J. Stat. Mech. **P05001**, 1742 (2011).
22. P. V. Hendriksen, S. Linderoth, and P. A. Lindgard, Phys. Rev. B **48**, 7259 (1993).
23. R. H. Kodama, J. Magn. Magn. Mater. **200**, 359 (1999).
24. K. N. Trohidou, in *Surface Effects in Magnetic Nanoparticles,* Ed. by D. Fiorani (Springer, 2005).
25. V. S. Leite and W. Figueiredo, Braz. J. Phys. **36**, 652 (2006).
26. V. Yu. Irkhin, A. A. Katanin, and M. I. Katsnel'son, Fiz. Met. Metalloved. **79**, 65 (1995).
27. A. A. Katanin and V. Yu. Irkhin, Phys. Usp. **50**, 613 (2007).
28. A. N. Ignatenko, A. A. Katanin, and V. Yu. Irkhin, JETP Lett. **97**, 209 (2013).

Translated by V. Astakhov